

Electron-Diffraction Evidence for Threefold Coordination in Amorphous Hydrogenated Carbon Films

D. R. McKenzie

School of Physics, University of Sydney, Sydney, New South Wales 2006, Australia

and

L. C. Botten

*School of Mathematical Sciences, The New South Wales Institute of Technology, Broadway,
New South Wales 2007, Australia*

and

R. C. McPhedran

School of Physics, University of Sydney, Sydney, New South Wales 2006, Australia

(Received 9 August 1982)

An electron-diffraction analysis is presented of the structure of amorphous hydrogenated carbon prepared from a dc magnetron glow discharge in argon-acetylene mixtures. On the basis of the evidence provided by the reduced intensity function, the atomic radial distribution function, and a reconstruction of the reduced intensity function based on a graphite layer model, it is concluded that such films exhibit a threefold coordinated structure with only slight correlation in the positions of two-dimensional layers.

PACS numbers: 61.40.Df, 61.14.Fe, 68.55.+b

Carbon films deposited from glow discharges containing hydrocarbons are remarkable in their apparent dissimilarity to carbon films produced by other means, such as evaporation or sputtering of graphite. They are quite transparent to visible light and have very high electrical resistivities.¹ These characteristics among others have led to the conjecture²⁻⁴ that such films contain fourfold coordinated carbon, as in diamond. However, this model is not universally accepted.^{5,6}

It is important to distinguish between films produced with and without impact of ions during their growth. The former may be quite hard and are often called "*i* carbon,"⁷ whereas the latter are comparatively soft, and have been termed "polymeric."⁸ Films of both kinds have many applications; for example, as an insulating film in microelectronics or as a coating for fusion-reactor-vessel wall linings.⁹

Here, we investigate polymeric films deposited onto substrates at ambient temperature from a dc magnetron¹⁰ glow discharge containing 1 Pa partial pressure of argon and various partial pressures (0.2, 0.8 Pa) of acetylene. We present the results of an electron-diffraction study of the films, both as prepared and after heat treatment in vacuum at 500 °C. To our knowledge, diffraction techniques have not until the present time given unequivocal information as to their structure (for a review see Anderson¹¹).

We obtained diffraction patterns of unsupported fragments of film, of thicknesses 20 to 100 nm,

in random orientation with 100-keV electrons on photographic film and determined the intensity $I(s)$ as a function of $s = 4\pi\sin\theta/\lambda$ using a microdensitometer. To assist in the interpretation, we also obtained traces for powdered graphite and for films prepared by dc sputtering in argon from graphite and by evaporation in vacuum using an electron beam gun. We define the reduced intensity function as

$$I_0(s) = I(s)/B(s) - 1, \quad (1)$$

where $B(s)$ is a background representing the scattering which would be observed from the same film in the absence of any structure. $B(s)$ contains the atomic form factor and so our function $I_0(s)$ corresponds to the function $F(s)/s$, defined by Moss and Graczyk.¹² We then calculate the atomic radial distribution function

$$4\pi r\Delta(r) = (2/\pi) \int_0^{s_0} s I_0(s) \exp(-as^2) \sin sr ds \quad (2)$$

using a fast Fourier-transform algorithm. Typically data are available up to $s = s_0$ of the order of 15 \AA^{-1} and so it is necessary to include a suitable exponential term in order to diminish the termination effect caused by the finite data set.

The experimental variation of $I_0(s)$ for the films is shown in Fig. 1. Figure 1(a) gives a diffraction pattern for a powdered graphite sample, with line strengths and positions for crystalline graphite indicated by vertical bars. Principal reflections are labeled. Note that the (0002) reflection observed is considerably weaker than that calculated. However, diffraction patterns obtained

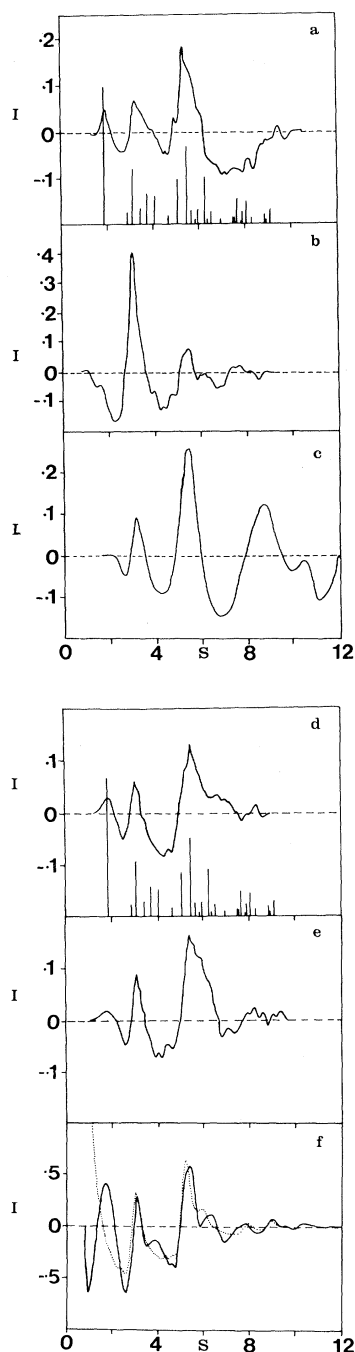


FIG. 1. The reduced intensity function as a function of scattering vector s in inverse angstroms for (a) powdered graphite with the expected positions of peaks and their relative intensities shown up to $s = 9.6 \text{ \AA}^{-1}$ (principal peaks are labeled); (b) a carbon film prepared by sputtering graphite in argon; (c) a carbon film prepared by electron beam evaporation; (d) a $a\text{-C:H}$ film as prepared, with graphite reflections shown; (e) the film of (d) after heat treatment; (f) a calculation of the reduced intensity function for one (dotted curve) and two (solid curve) threefold coordinated layers.

from other areas of the specimen showed much stronger (0002) reflections, with some weaker lines absent. This variability of the diffraction pattern is due to preferred orientation effects (or texturing) in the sample.

Specimens of amorphous hydrogenated carbon films were finely divided, and diffraction patterns were taken from fragments of unsupported film. We have confirmed that this method of preparation almost entirely eliminates orientation effects.

The carbon film of Fig. 1(b) was prepared by sputtering graphite on a dc magnetron containing 1 Pa of pure argon,^{13,14} at a current density of 15 A m^{-2} . It has a resistivity of $8.3 \times 10^{-3} \text{ } \Omega \text{ cm}$ and is dark in appearance. These properties are consistent with the diffraction pattern, which shows lines characteristic of microcrystalline graphite.

The film of Fig. 1(c) was prepared by electron-beam evaporation of graphite in vacuum. Its diffraction pattern differs remarkably from that of Fig. 1(b). Note the absence of subsidiary features around principal maxima, and the symmetric shape of the latter. This diffraction pattern is analogous to that of amorphous silicon, which has been successfully modeled by a random tetrahedral (fourfold coordinated) network.^{15,16} Kakinoki *et al.*¹⁷ have interpreted a comparable pattern using a combination of threefold and fourfold coordinated regions.

The film of Fig. 1(d) is an amorphous hydrogenated carbon film prepared in 0.2 Pa of acetylene. Its resistivity is greater than $10^8 \text{ } \Omega \text{ cm}$. Note the graphitic character of the diffraction pattern with asymmetric principal maxima and many small features coinciding with the graphite reflections of Figs. 1(a) and 1(b). The maxima at the lowest value of s corresponds to the (0002) reflection of graphite, but is also present in the diffraction pattern of many hydrocarbon polymers such as polyethylene.¹⁸ We interpret this peak as arising partly from the hydrocarbon polymers contained⁶ in $a\text{-C:H}$ and partly from two or more threefold coordinated layers with approximately the same spacing as in graphite.

The diffraction pattern of Fig. 1(e) corresponds to the film of Fig. 1(d) after 1 h of heat treatment in vacuum at $500 \text{ }^\circ\text{C}$. The subsidiary peaks corresponding to reflections of graphite have become more pronounced, indicating an increase in the size of the threefold coordinated microcrystalline regions. The weakening of the (0002) peak is accompanied by the disappearance of absorption due to CH_3 and CH_2 groups from the infrared trans-

mission spectrum.⁶

As an aid to the interpretation of the diffraction patterns of Figs. 1(d) and 1(e), we calculated the function

$$I_0(s) = \frac{1}{N} \sum_{i \neq j} \frac{\sin(sr_{ij})}{sr_{ij}} \exp(-2W) \quad (3)$$

for a crystallite of graphite (of side N_1 unit cells in the layers and N_2 threefold coordinated layers high) containing N atoms. W is the Debye-Waller factor for carbon. The results are shown in Fig. 1(f), for $N_1 = 7$ and N_2 equal to 1 and 2. A combination $I_0(s)$ gives quite a good fit to the curves for α -C:H, reproducing the relative intensities of the major peaks, and their asymmetric shape as well as some of the minor features. Taking into account our remarks above attributing the peak in the (0002) position partly to hydrocarbon polymers, we require a low predicted intensity for this peak from the carbon network. This implies that a single layer is more common than two, but note that there must be a small occurrence of regions in which a number of layers are spatially correlated in order to predict the remaining subsidiary peaks characteristic of three-dimensional graphite.

The calculation of the radial distribution function (2) for the film after annealing (Fig. 2) is consistent with the model of threefold coordination. The first peak in $4\pi r\Delta(r)$ occurs at 1.40 Å, corresponding to the first-neighbor distance in graphite of 1.42 Å. (Note that for diamond first neighbors are at 1.54 Å.) The second peak is due in part to second neighbors at 2.46 Å and also to third neighbors at 2.84 Å. Because our technique at present does not allow us to sample beyond $s = 15 \text{ \AA}^{-1}$, the resolution of the curve is insufficient to separate the two peaks. A fourfold coordinated model, in the form either of diamond

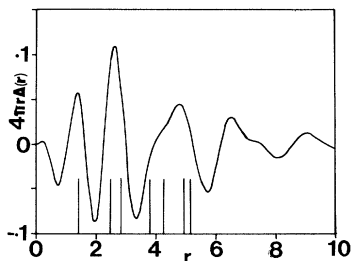


FIG. 2. The radial distribution function $4\pi r\Delta(r)$ as a function of distance r in angstroms. The interatomic distances of a threefold coordinated layer out to sixth neighbors are marked.

microcrystals^{2,4} or of a random tetrahedral network, is incompatible with Fig. 2. The former has a fourth-neighbor distance of 3.55 Å, while the latter has an important peak in the radial distribution function^{15,16} at 3.26 Å. Both these distances lie close to a deep minimum in the curve of Fig. 2.

We have obtained direct evidence of the polymer content in α -C:H, and its important contribution to the diffraction pattern. By placing a substrate at the entrance to the hot zone of the vacuum annealing furnace, we collected a deposit of condensed volatile material.⁶ We have obtained an electron-diffraction pattern of this distilled polymer. This pattern is generally similar to that of Fig. 1(d), having three principal peaks, the two at higher values being asymmetric. The values of s for the three peaks are 2.1 ± 0.3 , 3.4 ± 0.3 , and $5.6 \pm 0.5 \text{ \AA}^{-1}$. The position of the first of these peaks agrees within error with that of the corresponding peak of Fig. 1(d), confirming that the polymer material has a contribution to this peak.

Films of α -C:H prepared in high acetylene partial pressures (0.8 Pa) had diffraction patterns very similar to that of the polymer, but after annealing their diffraction patterns more closely resembled that of Fig. 1(e). These observations are consistent with polymer content in α -C:H which increases with acetylene partial pressure and decreases with annealing.

We have also deposited a film of α -C:H onto a substrate maintained at a temperature of 400 °C. The diffraction pattern of this film closely resembled that in Fig. 1(d), showing that threefold coordination persists at least up to substrate temperatures of 400 °C. It is interesting that the film prepared at this temperature was noticeably harder than ones prepared at room temperature.

In another work,⁶ we present additional evidence for the predominance of threefold coordination in annealed films. The use of optical sum rules has enabled us to show that about 46% of the carbon atoms in such films are threefold coordinated, and infrared spectroscopy shows that many of the remainder are bonded to hydrogen.

The material as prepared is likely to be two phase as has been suggested.¹⁰ One of the phases is a hydrocarbon polymer containing CH_3 and CH_2 groups, the other a carbon-rich network containing microcrystalline regions of threefold coordinated layers.

The authors thank Dr. D. J. H. Cockayne and Dr. N. Savvides for experimental assistance, and

acknowledge the financial support provided by the New South Wales Institute of Technology, His Royal Highness Prince Nawaf Bin Abdul Aziz of the Kingdom of Saudi Arabia, and the New South Wales Government through the Science Foundation for Physics within the University of Sydney.

¹B. Meyerson and F. W. Smith, *J. Non-Cryst. Solids* **35/36**, 435 (1980).

²S. Berg and L. P. Andersson, *Thin Solid Films* **58**, 117 (1979).

³L. Holland and S. M. Ojha, *Thin Solid Films* **58**, 109 (1979).

⁴S. Craig and G. L. Harding, *J. Vac. Sci. Technol.* **23**, 833 (1982).

⁵N. Wada, P. J. Gaezi, and S. A. Solin, *J. Non-Cryst. Solids* **35/36**, 543 (1980).

⁶D. R. McKenzie, R. C. McPhedran, N. Savvides, and L. C. Botten, to be published.

⁷C. Weissmantel, G. Reisse, H. J. Erler, F. Henny, K. Bewilogua, U. Ebersbach, and C. Schürer, *Thin Sol-*

id Films **63**, 315 (1979).

⁸K. Enke, *Thin Solid Films* **80**, 227 (1981).

⁹S. K. Das, M. Kaminsky, L. H. Rovner, J. Chin, and K. Y. Chen, *Thin Solid Films* **63**, 227 (1979).

¹⁰D. R. McKenzie and L. M. Briggs, *Solar Energy Mater.* **6**, 97 (1981).

¹¹D. A. Anderson, *Philos. Mag.* **35**, 17 (1977).

¹²S. C. Moss and J. F. Graczyk, *Phys. Rev. Lett.* **23**, 1167 (1969).

¹³D. R. McKenzie, N. Savvides, R. C. McPhedran, L. C. Botten, R. P. Netterfield, and P. J. Martin, in *Proceedings of the Max Born Centenary Conference, Edinburgh, SPIE Conference Series, 1982* (to be published).

¹⁴D. R. McKenzie, R. C. McPhedran, L. C. Botten, and R. P. Netterfield, *Appl. Opt.* **21**, 3615 (1982).

¹⁵D. E. Polk, *J. Non-Cryst. Solids* **8/10**, 19 (1972).

¹⁶J. F. Graczyk, *Phys. Status Solidi (a)* **55**, 231 (1979).

¹⁷J. Kakinoki, K. Katada, T. Hanawa, and T. Ino, *Acta Crystallogr.* **13**, 171 (1960).

¹⁸I. Voigt-Martin and F. C. Mijlhoff, *J. Appl. Phys.* **46**, 1165 (1975).